Nuclear Magnetic Resonance Relaxation of Glycogen H1 in Solution†

Wei Chen,*,‡ Xiao-Hong Zhu,‡ Malcolm J. Avison,§ and Robert G. Shulman‡

Departments of Molecular Biophysics & Biochemistry and Internal Medicine, Yale University School of Medicine, New Haven, Connecticut 06510

Received March 9, 1993; Revised Manuscript Received June 18, 1993®

ABSTRACT: The NMR relaxation properties of the H1 proton of oyster glycogen in D_2O and H_2O solutions have been studied using nonselective, semiselective, and selective inversion recovery and Hahn spin–echo pulse sequences. The data were analyzed in terms of an isotropic, rigid-rotor dipole–dipole model including cross-relaxation. At 8.4 T in D_2O, $\rho = 5.4 \pm 0.4$ s^{-1} and $\sigma = -4.5 \pm 0.4$ s^{-1}. The large, negative σ value is consistent with strong cross-relaxation and a long correlation time. The relaxation data can be explained by a single correlation time, $\tau_c = 2.7 \times 10^{-9}$ s, indicating significant internal mobility. With this value of τ_c, and assuming that the structure of the glucose moieties was the same as in α-D-glucose crystals, the dipole sum contributing to T_1 relaxation was calculated. The intra-ring relaxation was dominated by dipole fields from the H2 proton, but these only accounted for ~18% of the total relaxation. Most of the relaxation comes from inter-glucose relaxation. From modeling, this is dominated by the H4′ across the α-1,4-glycosidic bond. The H1 longitudinal relaxation rates were significantly enhanced in H_2O compared with D_2O. This enhancement is not due to direct dipolar interaction between H1 and bulk water. Transverse relaxation rates were not significantly enhanced in H_2O.

The polysaccharide glycogen is the main carbohydrate storage molecule in animals and humans, reaching concentrations of 60–100 mM (glucose equivalents) in muscle and 300–400 mM in liver. The primary structure consists of α-1,4-linked glucose chains containing 12–13 glucose residues, with α-1,6 branch points (Gunja-Smith et al., 1970).

The molecular weight of the glycogen molecule can reach 10^8. Despite this high molecular weight, the ^{13}C and ^1H resonances of glycogen are relatively sharp *in vitro*, indicating a high degree of internal mobility (Sillerud & Shulman, 1983; Zang et al., 1990a). Studies of the relaxation properties of the ^{13}Cl of glycogen suggest that there is significant internal motion. Thus Sillerud and Shulman found that the relaxation behavior of extracted rat liver glycogen *in vitro* could be explained by a rigid-rotor, isotropic dipole model with a single τ_c of 4.5 ns (Sillerud & Shulman, 1983). Furthermore, Zang et al. found that the ^{13}Cl T_1 of extracted rabbit liver glycogen could be described by a rigid-rotor dipolar model with a τ_c of 6 ns (Zang et al., 1990b). However, they obtained a better fit to the field dependence of ^{13}Cl T_1 and T_2 by assuming a distribution of correlation times, with an average value of 3.9 ns, and a small contribution from the molecular rotational correlation time, $\tau_M \approx 10^{-5}$ s (Zang et al., 1990b). Both of these studies indicate that the correlation time which dominates the $^{13}C1$–$^1H1$ dipolar interaction is therefore much shorter than the molecular rotational correlation time. The low sensitivity of ^{13}C NMR limits the accuracy of the measurements and the analysis of relaxation properties, particularly where multiexponential relaxation is present.

^1H NMR of glycogen has much greater sensitivity because of the higher magnetogyric ratio and high natural abundance of ^1H compared with ^{13}C. Zang et al. have shown that many of the ^1H resonances of extracted rabbit liver glycogen dissolved in D_2O can be resolved *in vitro* (Zang et al., 1990a, 1991). They also used 2D homonuclear (^1H–^1H) and heteronuclear (^{13}C–^1H) COSY to assign these resonances (Zang et al., 1991). At 8.4 T using nonselective excitation, the T_1 of glycogen H1 was 1.2 s and the T_2 was 29 ms in D_2O (Zang et al., 1990a).

The present study investigated the *in vitro* relaxation properties of the glycogen H1 resonance in relatively low molecular weight glycogen as a step toward understanding the molecular mechanisms which dominate ^1H relaxation in glycogen. Selective, semiselective, and nonselective excitation of the H1 resonance was used to evaluate the cross-relaxation between H1 and other protons.

THEORY

In contrast to other relaxation mechanisms, dipolar relaxation includes pathways involving $\Delta m = 0$ and $\Delta m = 2$ transitions. The identification of effects of these transitions is diagnostic of a dipolar contribution to the relaxation process under scrutiny. The relative importance of the zero and double quantum transitions depends on the correlation time τ_c. Two consequences of the presence of these terms are the observation of a nuclear Overhauser enhancement following irradiation of one of the interacting nuclei (Noggle & Schirmer, 1971) and the departure from monoexponential recovery of the spin–lattice relaxation of one of the interacting nuclei following its selective inversion (Freeman et al., 1974).

For the case of two homonuclear spins, I and S (*i.e.*, $\gamma_I = \gamma_S = \gamma$), and dipolar relaxation, the time dependences of z magnetizations I_z and S_z are

$$d(I_z - I_0)/dt = -(I_z - I_0)\rho_I - (S_z - S_0)\sigma_{IS} \quad (1a)$$

$$d(S_z - S_0)/dt = -(S_z - S_0)\rho_S - (I_z - I_0)\sigma_{SI} \quad (1b)$$

in which I_0 and S_0 are the equilibrium values of I_z and S_z and

† This work was supported by the National Institutes of Health from NIDDK Grant DK43146 to R.G.S. and Biomedical Research Support Grant RR05358 to M.J.A.

* Address correspondence to this author: Yale University School of Medicine, 125 Magnetic Resonance Center (MRC), 333 Cedar Street, P.O. Box 3333, New Haven, CT 06510. Telephone: (203) 785-6622. Fax: (203) 785-6643.

‡ Department of Molecular Biophysics & Biochemistry.

§ Department of Internal Medicine.

® Abstract published in *Advance ACS Abstracts*, August 15, 1993.

0006-2960/93/0432-9417$04.00/0

where (assuming for simplicity that $\rho_I = \rho_S = \rho$, $\sigma_{IS} = \sigma_{SI} = \sigma$)

$$\rho = 2W_1 + W_2 + W_0 \quad (2)$$

$$\sigma = W_2 - W_0 \quad (3)$$

W_1, W_0, and W_2 are the rates for single, zero, and double quantum transitions where

$$W_1 = (3/20)(\gamma^4\hbar^2/r^6)[\tau_c/(1 + \omega_I^2\tau_c^2)] \quad (4)$$

$$W_0 = (1/10)(\gamma^4\hbar^2/r^6)[\tau_c/(1 + (\omega_I - \omega_S)^2\tau_c^2)] \quad (5)$$

$$W_2 = (3/5)(\gamma^4\hbar^2/r^6)[\tau_c/(1 + (\omega_I + \omega_S)^2\tau_c^2)] \quad (6)$$

The general solution of eq 1 is given by

$$I_z(t) = I_0[1 + C_1e^{-(\rho+\sigma)t} + C_2e^{-(\rho-\sigma)t}] \quad (7)$$

The values of C_1 and C_2 depend on $I_z(0)$ and $S_z(0)$. We consider the following two cases.

(*a*) *Nonselective Inversion.* Following equal inversion of both I and S, eq 7 reduces to

$$I_z(t) = I_0[1 - C_1e^{-(\rho+\sigma)t}] \quad (8)$$

and the recovery of I_z to equilibrium is monoexponential with a nonselective T_1:

$$T_{1,ns} = (\rho + \sigma)^{-1} \quad (9)$$

(*b*) *Selective Inversion.* The recovery of I_z following the selective inversion of spin I is biexponential (eq 7, with $C_1 = C_2 = -1$) for complete inversion of I. In the limit of $\omega\tau_c \gg 1$, the W_0 term dominates both ρ and σ so that $\rho \approx -\sigma$. In the initial period following inversion, $\rho + \sigma \rightarrow 0$, $e^{-(\rho+\sigma)t} \approx 1$, and the early recovery of I is dominated by a selective T_1:

$$T_{1,s} = (\rho - \sigma)^{-1} \quad (10)$$

In summary, the I_z recovery following nonselective inversion is monoexponential with time constant $T_{1,ns} = (\rho + \sigma)^{-1}$ over the whole recovery. However, the recovery of I_z following its selective inversion is initially rapid, with time constant $T_{1,s} = (\rho - \sigma)^{-1}$, and subsequently is slower with time constant $(\rho + \sigma)^{-1}$. Measurement of the recovery following selective inversion of I therefore depends upon the values of $(\rho + \sigma)^{-1}$ and $(\rho - \sigma)^{-1}$.

W_0, W_1, and W_2 are functions of the correlation time of the dipolar interaction τ_c (eqs 4–6). We can therefore gain information about the molecular motion dominating the relaxation process from the relaxation rates. From eqs 2–6, 9, and 10, we obtain

$$1/T_{1,ns} = (1/10)(\gamma^4\hbar^2/r^6)[3J(\omega) + 12J(2\omega)] \quad (11)$$

and

$$1/T_{1,s} = (1/10)(\gamma^4\hbar^2/r^6)[2J(0) + 3J(\omega)] \quad (12)$$

where $J(\omega) = \tau_c/[1 + (\omega\tau_c)^2]$. Also (Abragam, 1985),

$$1/T_{2,ns} = (1/10)(\gamma^4\hbar^2/r^6)[3J(0) + 5J(\omega) + 2J(2\omega)] \quad (13)$$

where $T_{2,ns}$ is the T_2 measured using nonselective pulses. From eqs 11 and 13, we obtain

$$T_{1,ns}/T_{2,ns} = \frac{3J(0) + 5J(\omega) + 2J(2\omega)}{3J(\omega) + 12J(2\omega)} \quad (14)$$

while eqs 11 and 12 give

$$T_{1,ns}/T_{1,s} = \frac{2J(0) + 3J(\omega)}{3J(\omega) + 12J(2\omega)} \quad (15)$$

Clearly, for a fixed ω (i.e., fixed field strength), $T_{1,ns}/T_{2,ns}$ and $T_{1,ns}/T_{1,s}$ are dependent only on τ_c. We can therefore obtain independent measurements of τ_c by measuring $T_{1,ns}$, $T_{1,s}$, and $T_{2,ns}$ and using eqs 14 and 15.

METHODS

Sample Preparation. Glycogen from the same batch of commercially available glycogen (Oyster Glycogen Type II, Sigma cat. no. G-8751) was dissolved in D_2O or H_2O to 370 mM. Both solutions contained 2 mM NaN_3 as a preservative and were adjusted to pH ~7 by adding NaOH. A single 0.5-mL sample of each solution was transferred to a 5-mm NMR tube and used for all measurements.

NMR Methods. ^1H spectra were collected using a Bruker AM 360 (8.4 T, operating at 360 MHz for ^1H) equipped with a 5-mm ^1H probe. Values of the T_1 relaxation time were determined using inversion recovery sequences with nonselective, semiselective, or selective inversions as indicated. T_2 values were determined using a standard Hahn spin–echo sequence. A 1–1 sequence (Hore, 1983) was used for all semiselective pulses. The interpulse delay was 1.78 ms, such with the RF carrier on the water resonance maximal excitation of the H1 resonance 281 Hz downfield was achieved. Because of this delay, the semiselective sequence also provided 50–80% inversion of the H2–H5 envelope on the upfield side of water. Thus the semiselective inversion pulse behaves in a manner similar to the hard pulse, except that the water magnetization is unperturbed. A DANTE (Morris & Freeman, 1978) train was used for selective inversions. It consisted of 70–80 pulses spaced 100–300 μs apart to give selective H1 inversion with a negligible effect on the water and other glycogen resonances. All spectra were run fully relaxed (TR = 15 s (repetition time) for glycogen in D_2O and 10 s for glycogen in H_2O) at 37 °C. The 90° pulse width was between 8 and 9 μs.

Analysis of Relaxation Curves. All relaxation curves were first fit to the monoexponential recovery function (eq 8). If the sum of the residuals exceeded that expected on the basis of the noise amplitude in the spectra, or a semilog plot revealed two linear regions of different slopes, then data were analyzed differently depending upon whether the measurements were in D_2O or H_2O. For studies in D_2O, where chemical exchange does not complicate the analysis of the relaxation curves, the data were fit to the more general solution given in eq 7. The 95% confidence limits of the values of $(\rho + \sigma)$ and $(\rho - \sigma)$ obtained from the fits were determined using a Monte Carlo estimation based on the noise amplitude in the spectra and the estimated error in base-line correction (Press et al., 1989). In the case of multiexponential relaxation in H_2O, where the effects of chemical exchange may complicate the time course of later H1 recovery, we determined the initial rate of recovery from biexponential curve fitting to eq 7 and confirmed the initial rate from the slope of semilog plots during the first 50–70 ms following selective inversion.

RESULTS

Figure 1a shows the ^1H spectrum of glycogen in D_2O obtained following a nonselective $\pi/2$ pulse at 360 MHz and 37 °C. The resonance assignments follow Zang et al. (1991). The H1 proton gives rise to the downfield resonance at 5.38 ppm with a line width of ~15 Hz. Figure 1b shows the

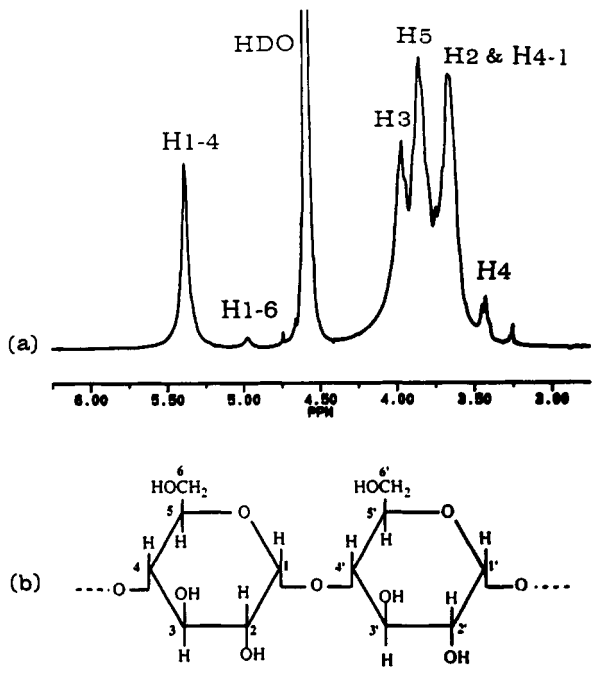

FIGURE 1: (a) ^{1}H spectrum of glycogen in D_2O collected using a pulse–acquire sequence at 360 MHz. (b) Structure of two glucose monomer subunits in α-1,4-linkage showing proton numbers.

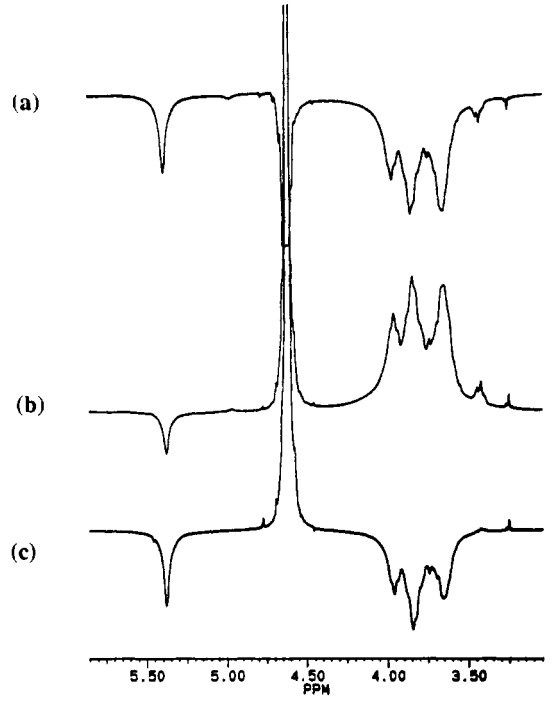

FIGURE 2: ^{1}H spectra of glycogen in D_2O at 360 MHz obtained following (a) nonselective inversion of all spins (including HDO) by a hard π pulse; (b) selective inversion of the H1 resonance using a DANTE train; and (c) semiselective inversion pulse optimized to invert the H1 resonance while leaving the HDO magnetization at equilibrium. Note that the upfield H2–H5 envelope is also inverted by 50–80%. For details of the pulse sequences used, see Methods.

structure of two glucose monomer subunits in α-1,4-linkage with the conventional proton numbering.

Effect of Inversion Pulses. Figure 2 compares the effects of different inversion sequences on the ^{1}H resonances of glycogen. Nonselective inversion of all spins (including HDO) by a hard π pulse is effective across all of the glycogen resonances as shown in Figure 2a, although the inversion is incomplete due to B_1 inhomogeneity. Figure 2b shows the spectrum obtained immediately following selective inversion of the H1 resonance using a DANTE train. The selective inversion has no direct effect on the other resonances. The inversion of H1 is incomplete due to T_2 losses during the DANTE train and B_1 inhomogeneity. The semiselective inversion pulse (Figure 2c), optimized to invert the H1 resonance while leaving the HDO magnetization at equilibrium, leads to almost complete inversion of the H1 resonance and the upfield glycogen resonances between 4.1 and 3.6 ppm. However, the H1–6 (4.99 ppm) and free-end H4 (3.44 ppm) resonances were weaker in comparison with Figure 2a,b due to the excitation profile of the semiselective inversion pulse.

T_1 of Glycogen H1. Figure 3 shows the T_1 recovery of glycogen H1 in D_2O following nonselective and semiselective inversion. In both cases the relaxation is monoexponential. Fitting to eq 8 gave $T_{1,ns} = 1.14 \pm 0.05$ s for nonselective and $T_{1,ss} = 1.05 \pm 0.04$ s for semiselective inversion. That $T_{1,ns} \approx T_{1,ss}$ is to be expected given the near-complete inversion of the H2–H5 protons by the semiselective pulse (Figure 2c) and indicates that the semiselective inversion pulse is equivalent to a nonselective inversion of all of the protons involved in the relaxation of glycogen H1 in D_2O. Furthermore, it suggests that, in sequences where water suppression is important, the semiselective inversion may be used instead of a nonselective inversion to measure a $T_{1,ss}$ which is equivalent to the $T_{1,ns}$.

Relaxation of the glycogen H1 in D_2O following selective inversion (Figure 4) shows pronounced biexponential behavior, with a much faster initial recovery than after nonselective inversion. The solid line in Figure 4 is the best fit to eq 7. We constrained the value of $(\rho + \sigma)$ to be within the 99% confidence interval of $(\rho + \sigma)$ determined from the monoexponential recovery following nonselective inversion. The fit gave $(\rho + \sigma) = 1.2 \pm 0.2$ s^{-1} and $(\rho - \sigma) = 9.9 \pm 0.7$ s^{-1}, and thus $T_{1,s} = 0.10 \pm 0.01$ s. Using the value of $(\rho + \sigma)$ from the nonselective inversion and $(\rho - \sigma)$ from the selective inversion, we obtain $\rho = 5.4 \pm 0.4$ s^{-1} and $\sigma = -4.5 \pm 0.4$ s^{-1}, where the confidence limits for ρ and σ are dominated by the uncertainty in $(\rho - \sigma)$. Consequently $\rho \approx -\sigma$, indicating that the cross-relaxation of glycogen H1 with other protons is dominated by the zero quantum transition, W_0. This is consistent with $\omega\tau_c \geq 1$.

Following selective inversion, the initial rates of recovery are the same in H_2O and D_2O, i.e., $T_{1,s}$ is the same in H_2O and D_2O (see Table I). Following semiselective inversion in H_2O, the recovery of H1 is monoexponential as in D_2O but has $T_{1,ss} = 0.31 \pm 0.01$ s (Figure 5), which is appreciably shorter than the value of 1.05 ± 0.04 s in D_2O. Table I summarizes the T_1 results for the glycogen H1 proton in H_2O and D_2O following selective (H1 only), semiselective (H1 and H2–H5), and nonselective inversions.

T_2 of Glycogen H1. The results of T_2 measurements of glycogen H1 are summarized in Table II. The T_2 values measured using a nonselective refocusing pulse in D_2O and a semiselective refocusing pulse in H_2O were not significantly different (35 ± 3 ms in D_2O vs 38 ± 3 ms in H_2O). The T_2 measured in D_2O using a semiselective refocusing pulse was slightly longer (48 ± 4 ms).

DISCUSSION

Given the long molecular correlation time ($\tau_M \approx 10^{-5}$ s; Zang et al., 1990b) expected for a molecule size of glycogen, its ^{1}H resonances are surprisingly sharp in solution, indicating a large amount of internal motion. The relaxation measurements performed in this study can give insight into the nature of these internal motions and suggest methods for gaining useful information about the solution structure of the glycogen molecule.

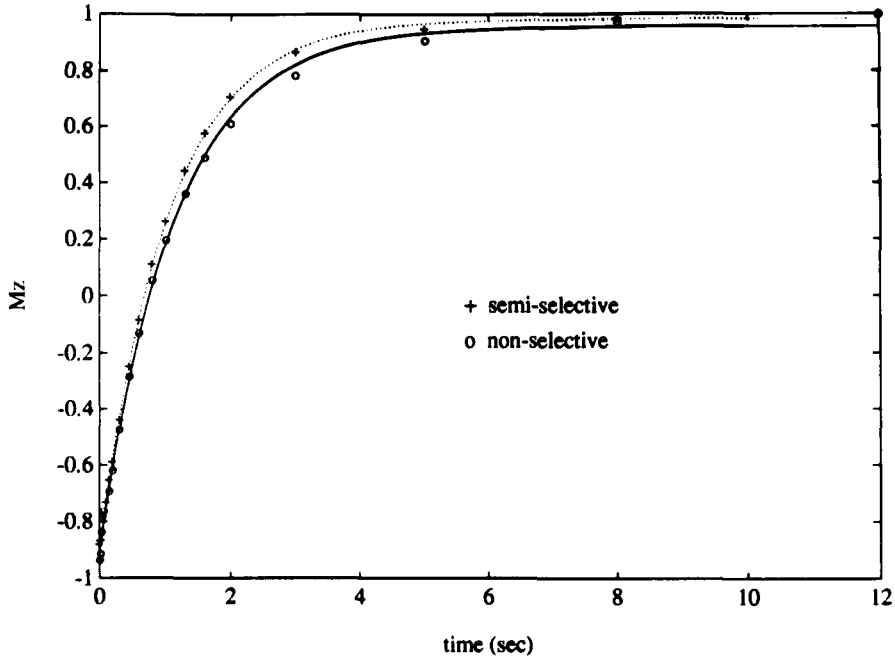

FIGURE 3: Recovery of glycogen H1 in D_2O following nonselective (O) and semiselective (+) inversion of all glycogen protons. Points are measured data. The lines are the best fit to eq 8 in both cases.

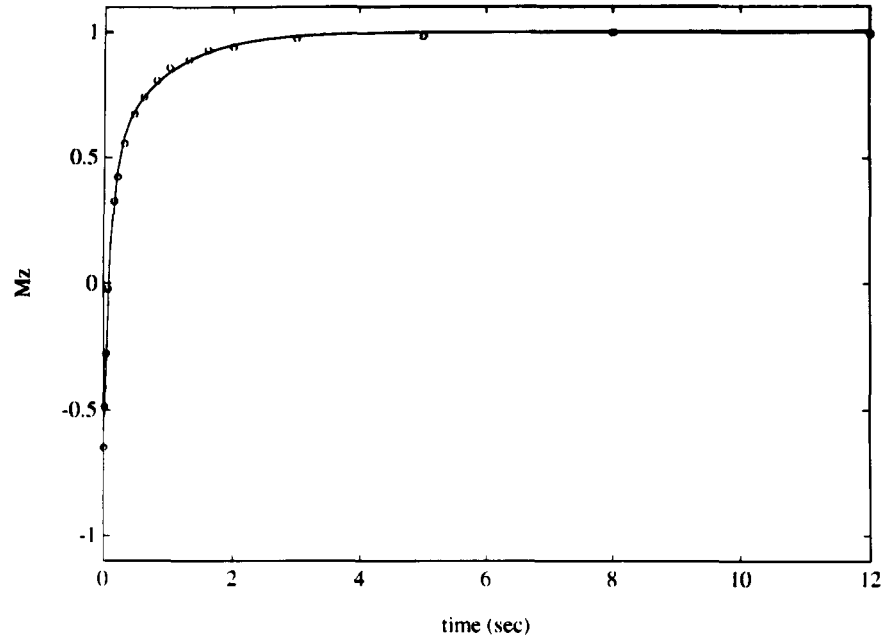

FIGURE 4: Recovery of glycogen H1 in D_2O following selective inversion of H1. Points are measured data. The solid line is the best fit to eq 7.

Table I: Summary of T_1 Relaxation Times of Glycogen H1 Proton at 310 K and 360 MHz[a]

pulse type	T_1 (s) in D_2O	T_1 (s) in H_2O
nonselective	1.14 ± 0.05	
semiselective	1.05 ± 0.04	0.31 ± 0.01
selective	0.10 ± 0.01[b]	0.09 ± 0.01[b]

[a] Errors are 95% confidence limits. [b] Initial relaxation rate (details in text).

Table II: Summary of T_2 Relaxation Times of Glycogen H1 Proton at 310 K and 360 MHz[a]

pulse type	T_2 (ms) in D_2O	T_2 (ms) in H_2O
nonselective	35 ± 3	
semiselective	48 ± 4	38 ± 3

[a] Errors are 95% confidence limits.

The dependence of $T_{1,ns}/T_{2,ns}$ on τ_c for ν = 360 MHz is shown in Figure 6a (from eq 14). In D_2O, $T_{1,ns}/T_{2,ns}$ = 32 for the H1 proton, corresponding to $\tau_c = 2.8 \times 10^{-9}$ s. Figure 6b shows the calculated dependence of $T_{1,ns}/T_{1,s}$ on τ_c for ν = 360 MHz (from eq 15). In D_2O, $T_{1,ns}/T_{1,s}$ = 11 for the H1 proton, corresponding to $\tau_c = 2.5 \times 10^{-9}$ s, in excellent agreement with the value of τ_c obtained from $T_{1,ns}/T_{2,ns}$. This agreement provides strong support for our assumption of a purely dipolar relaxation mechanism of glycogen in D_2O. Further support comes from the measured value of $T_{1,ns}$ in D_2O at ν = 500 MHz. Using the calculated τ_c of 2.7×10^{-9} s (the mean of the values for τ_c obtained above), we expect the $T_{1,ns}$ value at 500 MHz to be 2.1 s. The measured value was 2.0 s.

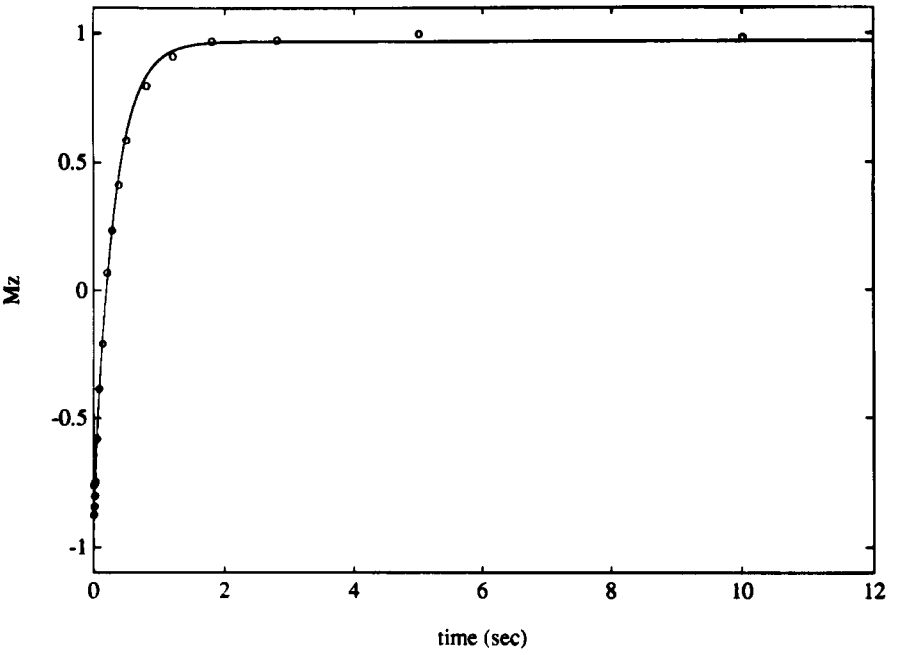

FIGURE 5: Recovery of glycogen H1 following semiselective inversion of H1 in H_2O. The time course of the recovery was fit to eq 8, giving $T_{1,ss} = 0.31 \pm 0.01$ s.

Table III: H1–H*i* Internuclear Distances and Corresponding Relaxation Rates for the Intra-Ring Protons of Glucose

interaction	r_i (Å)	$(\rho + \sigma)$ (s^{-1})
H1–H2	2.383	0.133
H1–H3	3.855	7.428×10^{-3}
H1–H4	3.981	6.125×10^{-3}
H1–H5	3.622	1.080×10^{-2}
H1–H6	5.434; 4.439	9.469×10^{-4}; 3.187×10^{-3}
H1–OH_2	3.4517	
total (H2–H6)[a]		0.162

[a] Sum of the rate constants for the H1–H2 through H1–H6 interactions.

Once we know the internuclear distances between H1 and the *i*th proton (r_i) and the appropriate correlation time τ_c, we can calculate the contributions of the intra-ring protons to the dipolar relaxation rate of H1 following nonselective inversion ($1/T_{1,ns}$) and the initial relaxation rate following selective inversion ($1/T_{1,s}$) in D_2O. From eqs 2–6, 9, and 10, we have

$$(T_{1,ns})^{-1} = \sum_i (\rho + \sigma)_i = \sum_i 2(W_1 + W_2)_i$$
$$= (3/10)\gamma^4\hbar^2[J(\omega,\tau_c) + 4J(2\omega,\tau_c)]\sum_i r_i^{-6} \quad (16)$$

$$(T_{1,s})^{-1} = \sum_i (\rho - \sigma)_i = \sum_i 2(W_1 - W_0)_i$$
$$= (1/10)\gamma^4\hbar^2[3J(\omega,\tau_c) + 2J(0,\tau_c)]\sum_i r_i^{-6} \quad (17)$$

Table III compiles the distances used to calculate individual intra-ring dipolar interactions and the $(\rho + \sigma)_i$ (i.e., contributions to $1/T_{1,ns}$) of these interactions, using $\tau_c = 2.7 \times 10^{-9}$ s. The r_i values were calculated from the nuclear coordinates of the protons in α-D-glucopyranose using Chem3D molecular modeling software (Cambridge Scientific). The nuclear coordinates used were those of Brown and Levy (1965) obtained by neutron diffraction. The dominant intra-ring interaction is that between H1 and H2, followed by weaker H1–H3 and H1–H5 interactions. The total dipolar contribution from all of these intra-ring protons is 0.162 s^{-1} for $1/T_{1,ns}$. This is only ~18% of the experimental rate observed in D_2O (0.88 ± 0.04 s^{-1}).

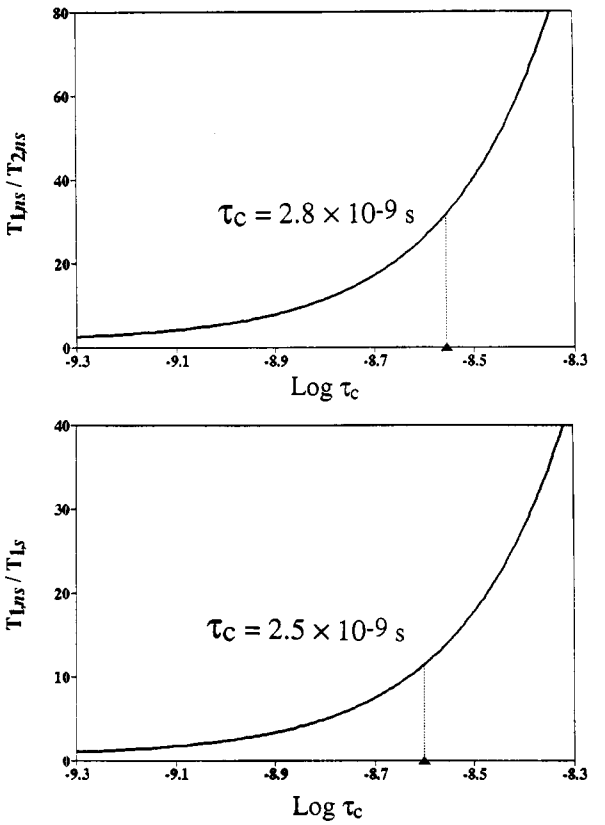

FIGURE 6: (a, top) Dependence of $T_{1,ns}/T_{2,ns}$ on τ_c calculated from eq 14. (b, bottom) Dependence of $T_{1,ns}/T_{1,s}$ on τ_c calculated from eq 15.

If the discrepancy is made up with one additional inter-ring dipolar interaction, the internuclear distance required for the interaction is 1.8 Å. Such a distance is less than the H–H van der Waals sum, suggesting that other interactions may play a role. Nonetheless, there are indications that the H1–H4′ distance ($r_{14'}$) may be unusually short. Goldsmith et al. found that the glucose heptamer maltoheptose bound to glycogen phosphorylase adopts a helical structure (Goldsmith et al., 1982). Assuming that this structure resembles the native

glycogen structure, they proposed a similar helical structure for the 13-mers which constitute the principal feature of the secondary structure of glycogen, with torsion angles for the C1–O1–C4′ glycosidic linkages of $\phi = -15°$ and $\psi = -15°$. This conformation is stabilized by a good inter-ring O2–O3′ hydrogen bond. Using these values, and the glucose coordinates of Brown and Levy (1965), we estimate an H1–H4′ distance of 1.8 Å in this structure, in agreement with the distance required to explain our relaxation data. Inclusion of additional interactions in our analysis would increase the required r_{14}' distance. Such interactions might be revealed by NOESY and ROESY experiments. However, given the extremely rapid fall-off of the H1–H4′ interaction's contribution to relaxation as $r_{14'}$ is increased, it is unlikely that other interactions within an individual glycogen 13-mer have sufficient strength to compensate for any significant increase in $r_{14'}$. Thus, if the ^1H–^1H distances are constrained to be no less than van der Waals sum (2.2 Å), inclusion of even three additional dipolar interactions would be insufficient to explain the observed relaxation rates. Since the H1 proton is located on the exterior of the proposed helix, an interesting possibility is that dipolar relaxation by nearby protons on adjacent chains may contribute significantly to the H1 relaxation rate. Clearly H1 relaxation is dominated by inter- rather than intra-ring interactions, and the dominant intra-chain, inter-ring interaction is with H4′.

In an earlier study, Zang et al. reported that it was necessary to include an additional molecular correlation time, τ_m, to explain the *in vitro* field dependence of the relaxation behavior of rabbit liver glycogen ^{13}Cl (Zang et al., 1990b). In the present study, the field dependence of the relaxation behavior of oyster glycogen $^1H1$ is fully explained by a single correlation time, $\tau_c = 2.7 \times 10^{-9}$ s. The τ_c calculated by Zang et al. from the value of T_1/T_2 (=37.9) for $^{13}C1$ assuming a rigid-rotor nearest-neighbor (RRNN) model is 3.1 ns, in good agreement with the present study. Both of these values for τ_c are also in agreement with several ^{13}C NMR studies in which the τ_c values for the $^{13}C1$ resonance calculated using an RRNN model were 4.5 (Sillerud & Shulman, 1983) and 6.4 ns (Zang et al., 1990b). Thus H1 and C1 have similar correlation times, even though the ^{13}Cl relaxation comes exclusively from the geminal H1 proton, while the $^1H1$ relaxation comes from other intra- and inter-ring interactions. We note that the long τ_c postulated by Zang et al. in a recent ^{13}C study was necessary to explain the short T_2 observed in that study. However, the T_2 of ^{13}Cl reported by Zang et al. is anomalously short compared with other measurements, and we are currently rechecking that measurement.

When H_2O is the solvent, the effects upon the H1 relaxation of direct cross-relaxation with H_2O, cross-relaxation with glycogen OH protons, and chemical exchange of the glycogen OH protons with H_2O must be considered. The correlation time for a direct H1–H_2O interaction would be much shorter ($\tau_c \approx 10^{-12}$ s) and inefficient for glycogen H1 relaxation. Our relaxation data in D_2O are consistent with a single τ_c of 2.7×10^{-9} s. Furthermore, the initial recovery following selective inversion of H1 is the same in H_2O and D_2O (i.e., $T_{1,s}$ is the same in D_2O and H_2O). It is therefore unlikely that there is significant direct cross-relaxation with H_2O.

From the crystallographic structure and the constraints on the solution structure imposed by our own relaxation measurements, the strongest dipolar interaction between H1 and any hydroxyl proton is very small compared with H1–H2 and H1–H4′. For the closest hydroxyl, $1/r^6_{(H1-OH)}$ is only 11% of $1/r^6_{(H1-H2)}$. However, the additional strong cross-relaxation of H2 by OH can lead to a more rapid relaxation of H1 following inversion of H1 and H2 (e.g., semiselective pulse inversion in H_2O versus D_2O) because the more rapid H2 relaxation leads to faster (monoexponential) H1 relaxation as a consequence of the strong H1–H2 W_0 term. Selective inversion of H1 in H_2O gave multiexponential relaxation with an initial rate indistinguishable from that in D_2O. Since the dominant cross-relaxation terms in the early stages of recovery are the same in both cases and there is no direct interaction with H_2O, we would expect the initial recovery in H_2O to have the same time constant as that in D_2O. The time constant for the slower phase of recovery is more difficult to analyze since it will be complicated by OH–H_2O chemical exchange, which in turn affects the time dependence of the H2 magnetization.

CONCLUSION

The relaxation rates of the glycogen H1 proton are explained by a model of rigid dipole–dipole interactions with an average isotropic $\tau_c = 2.7 \times 10^{-9}$ s. The dominant interactions are H1–H2 and H1–H4′. Comparison of the patterns of recovery of H1 following selective and nonselective inversion allowed us to determine the values $\rho = 5.4 \pm 0.4$ s^{-1} and $\sigma = -4.5 \pm 0.4$ s^{-1} for glycogen H1 in D_2O. The relatively large, negative σ value indicates strong cross-relaxation with the W_0 term dominating σ. Although long enough to allow significant cross-relaxation and a negative σ, τ_c is too short to be associated with the molecular correlation time, but rather is consistent with significant internal motion and is also consistent with the ^{13}Cl value of $\tau_c \approx 4.5$ ns previously reported.

REFERENCES

Abragam, A. (1985) in *Principles of Nuclear Magnetism*, pp 292, Oxford University Press, London.

Brown, G. M., & Levy, H. A. (1965) *Science 147*, 1038–1039.

Freeman, R., Hill, H. D. W., Tomlinson, B. L., & Hall, L. D. (1974) *J. Chem. Phys. 61*, 4466–4473.

Goldsmith, E., Sprang, S., & Fletterick, R. (1982) *J. Mol. Biol. 156*, 411–427.

Gunja-Smith, Z., Narshall, J. J., Mercier, C., Smith, E. E., & Wheelan, W. J. (1970) *FEBS Lett. 12*, 101–104.

Hore, P. J. (1983) *J. Magn. Reson. 55*, 283–300.

Morris, G. A., & Freeman, R. (1978) *J. Magn. Reson. 29*, 433–462.

Noggle, J. H., & Schirmer, R. E. (1971) in *The Nuclear Overhauser Effect. Chemical Applications*, Academic Press, New York.

Press, W. H., Flannery, B. P., Teukolsky, S. A., & Vetterling, W. T. (1989) in *Numerical Recipes in* Pascal, pp 572–590, Cambridge University Press, New York.

Sillerud, L. O., & Shulman, R. G. (1983) *Biochemistry 22*, 1087–1094.

Zang, L.-H., Rothman, D. L., & Shulman, R. G. (1990a) *Proc. Natl. Acad. Sci. U.S.A. 87*, 1678–1680.

Zang, L.-H., Laughlin, M. R., Rothman, D. L., & Shulman, R. G. (1990b) *Biochemistry 29*, 6815–6820.

Zang, L.-H., Howseman, A. M., & Shulman, R. G. (1991) *Carbohydr. Res. 220*, 1–9.